The Astrophysical Journal Letters, 803:L15 (5pp), 2015 April 20 doi:10.1088/2041-8205/803/2/L15

THE CONNECTION BETWEEN THE POSITRON FRACTION ANOMALY AND THE SPECTRAL FEATURES IN GALACTIC COSMIC-RAY HADRONS

Nicola Tomassetti[1] and Fiorenza Donato[2]
[1] LPSC, Université Grenoble-Alpes, CNRS/IN2P3, F-38026 Grenoble, France; nicola.tomassetti@lpsc.in2p3.fr
[2] Dipartimento di Fisica & INFN, Università di Torino, I-10125 Torino, Italy; fiorenza.donato@to.infn.it
Received 2014 December 12; accepted 2015 February 19; published 2015 April 14

ABSTRACT

Recent data on Galactic cosmic-ray (CR) leptons and hadrons gave rise to two exciting problems: on the lepton side, the origin of the rise of the CR positron fraction $e^+/(e^- + e^+)$ at ∼10–300 GeV of energy; on the hadron side, the nature of the spectral hardening observed in CR protons and nuclei at ∼TeV energies. The lepton anomaly indicates the existence of a nearby $e^\pm$ source. It has been proposed that high-energy positrons can be produced inside nearby supernova remnants (SNRs) via interactions of CR hadrons with the ambient medium. A distinctive prediction of this mechanism is a high-energy rise of the boron-to-carbon ratio, which has not been observed. It also requires *old* SNRs at work (with ineffective magnetic field amplification and slow shock speed) that cannot account for the CR hadronic spectra observed up to the knee energies (∼5 PeV). We propose a new picture where, in addition to such a nearby CR accelerator, the high-energy spectrum of CR hadrons is provided by the large-scale population of SNRs, younger on average, which can efficiently accelerate CRs up to the knee. Under this scenario, the spectral hardening of CR hadrons can be naturally interpreted as the transition between the two components. As we will show, our two-component model breaks the connection between the positron fraction and the boron-to-carbon ratio, which is now predicted to decrease with energy in accordance with the data. Forthcoming data from AMS will be crucial for testing this model.

Key words: acceleration of particles – cosmic rays – ISM: supernova remnants – nuclear reactions, nucleosynthesis, abundances

1. INTRODUCTION

The AMS collaboration has recently confirmed with high precision the cosmic-ray (CR) positron fraction anomaly previously observed by PAMELA (Adriani et al. 2009; Aguilar et al. 2013). The data show a rise of the fraction up to energies of ∼10–300 GeV, followed by a possible plateau at higher energies (Accardo et al. 2014), which cannot be described by conventional models of e^+ production by collisions of CR hadrons with the interstellar matter (ISM). In these models, the primary CRs (e.g., e^-, H, He, C, or O) are accelerated by supernova remnants (SNRs) via diffusive shock acceleration (DSA) mechanisms up to ∼PeV energies to power-law spectra $S \propto E^{-\nu}$. Their subsequent propagation is described by means of an energy-dependent confinement time $\tau_{\rm esc} \propto E^{-\delta}$ (or diffusion coefficient $K \propto E^{\delta}$), and their collisions with the ISM give rise to *secondary* CRs such as Li, Be, B, e^+, or $\bar{p}$ (Strong et al. 2007). At $E \gg$ GeV, this picture predicts power-law spectra for primary nuclei, $N_p \sim E^{-\nu-\delta}$, and decreasing secondary-to-primary ratios, e.g., the boron-to-carbon: B/C $\sim E^{-\delta}$, where $\delta \sim 0.3$–0.7, $\nu \sim 2.0$–2.4, and $\nu + \delta \approx 2.7$. The high-energy spectrum of CR leptons is further steepened by radiative losses, with characteristic timescale $\tau^{\rm rad}(E) \propto E^{-1}$. Given that all the positrons are from secondary origin, the positron fraction is expected to decrease similarly to other secondary-to-primary ratios, in remarkable contrast with the observations. Explanations of the rise may include either dark matter particle annihilation or decay or nearby astrophysical sources (Serpico 2011). Among the second class, it has been proposed that high-energy positrons may be produced through hadronic interactions of CR protons undergoing DSA inside *old* SNRs (Blasi 2009). Yet, if secondary positrons are produced and accelerated by this mechanism, other secondary species (such as B nuclei or $\bar{p}$) will also be produced from CR nuclei interacting with the gas. As shown by Mertsch & Sarkar (2009), this mechanism leads to an increase of the B/C ratio at $\gtrsim$100 GeV per nucleon. However, the current B/C ratio data decrease with energy, indicating that the *old* SNR scenario (hereafter OSNR) should be ruled out (Cholis & Hooper 2014).

On the other hand, the spectra of primary CR elements have been measured up to ∼PeV energies and beyond. Recent data on CR protons and nuclei revealed a remarkable spectral hardening at ∼TeV energies, which stimulated great interest (Blasi 2013). According to the PAMELA data on H and He (Adriani et al. 2011), the change of slope is located at $R \approx$ 230 GV of rigidity (i.e., momentum-to-charge ratio) with a very sharp transition, which is not seen by other experiments. While the sharpness of such breaks is under debate, the CR spectral hardening at $E \gtrsim 1$ TeV per nucleon is established by several experiments, such as CREAM and ATIC (Panov et al. 2009; Yoon et al. 2010). The proposed explanations invoke acceleration mechanisms (Ptuskin et al. 2013), diffusion effects (Blasi et al. 2012; Tomassetti 2012), or the superposition of local and distant sources (Vladimirov et al. 2012; Bernard et al. 2013; Thoudam & Horandel 2013).

In this Letter, we argue that the OSNR scenario is incomplete in order to account for the observations of CR hadron spectra. Whether the OSNR represents a single source or a population of sources with the characteristics required for producing secondary $e^\pm$ (i.e., low shock speed and damped magnetic fields), it cannot provide the flux of CR hadrons observed in the ∼TeV–PeV energy region, so an additional high-energy component of CR accelerators is needed. We propose a two-component SNR scenario where the high-energy part of the CR flux is provided by a Galactic ensemble of SNRs,

hereafter GSNR, that are on average younger and more efficient when accelerating primary hadrons at high energies (but are unable to accelerating secondaries). A key consideration is that the local flux of light CR nuclei depends on the large-scale structure of the Galaxy, reflecting the contribution of a large population of SNRs and their histories (Taillet & Maurin 2003). For $E \gtrsim 10$ GeV, their escape rate, $\tau_{\rm esc}^{-1}$, is generally larger than their spallation rate in the ISM $\tilde{\Gamma}^{\rm inel}$ so that their propagation is limited only by the size of the diffusion region. In contrast, light leptons are subjected to radiative cooling due to synchrotron radiation and inverse Compton scattering, which significantly limits the range that they can travel before reaching the solar system (Delahaye et al. 2010). Their characteristic distance is approximately $\lambda \sim \sqrt{\tau^{\rm rad} K} \propto E^{(\delta-1)/2}$, confined to ∼1 kpc at energies above ∼100 GeV (depending on the propagation parameters), which would legitimatize the OSNR approach. Thus, while the observed $e^{\pm}$ can be largely produced by only one or a few nearby sources, the total spectrum of CR protons and nuclei may well result as the sum of two SNR components: the nearby OSNR component, which would dominate the flux below ∼100 GeV, and the GSNR ensemble, which would provide the high-energy flux up to the knee. As we will show, a two-component model gives a good description of the primary CR spectral hardening, and it has an impact on the spectral shape of the B/C ratio, which is now determined to be the superposition of several contributions.

2. CALCULATIONS

The spectrum of CRs accelerated in SNRs is computed analytically using the linear DSA theory and including the secondary production terms due to hadronic interactions. We follow our calculations scheme in Tomassetti & Donato (2012), which has been proven to be equivalent to that of Mertsch (2009) and Mertsch & Sarkar (2014). In the shock rest-frame ($x = 0$), the upstream plasma flows in from $x < 0$ with speed u_1 (density n_1) and the downstream plasma flows out to $x > 0$ with speed u_2 (density n_2). The compression ratio is $r = u_1/u_2 = n_2/n_1$. For a nucleus with charge Z and mass number A, the DSA equation reads:

$$u\frac{\partial f}{\partial x} = D\frac{\partial^2 f}{\partial x^2} + \frac{1}{3}\frac{du}{dx}p\frac{\partial f}{\partial p} - \Gamma^{\rm inel} f + Q, \qquad (1)$$

where f is the phase space density, $D(p)$ is the diffusion coefficient near the SNR shock, u is the fluid velocity, and $\Gamma^{\rm inel} = c\beta n\sigma^{\rm inel}$ is the total destruction rate for fragmentation with the interaction cross-section $\sigma^{\rm inel}$. The ambient density n is assumed to be composed by 90% H and 10% He, similarly to the average ISM, in both sides of the shock. The source term is represented by Q. For primary nuclei $Q^{\rm pri} = Y\delta(x)\delta\left(p - p^{\rm inj}\right)$, i.e., the ambient particle injection occurs immediately upstream from the shock at momentum $p^{\rm inj} \equiv ZR^{\rm inj}$, where $R^{\rm inj} \equiv 1$ GV for all species. The Y constants are abundance factors, determined from the data. The source term for secondary fragments produced by spallation of heavier (k-labeled) nuclei is of the type $Q^{\rm sec} = \sum_k \Gamma_k^{\rm frag} f_k$, where the partial rates of fragmentation are $\Gamma_k^{\rm frac} = c\beta n\sigma_k^{\rm frag}$. Using the subscript $i = 1$ ($i = 2$) to indicate the quantities in the upstream (downstream) region, the downstream solution of each nucleus can be expressed as

$$f_2(x, p) = f_0 + \frac{rx}{u_2}\left(Q_0 - \Gamma_1^{\rm inel} f_0\right), \qquad (2)$$

where the subscript $i = 0$ indicates the quantities evaluated at the shock ($x = 0$), and $f_0(p)$ is given by

$$f_0(p) = \alpha\int_0^p \left(\frac{p'}{p}\right)^{\alpha} Q^{\rm pri}(p') e^{-\chi(p,p')}\frac{dp'}{p'} + \alpha\int_0^p \left(\frac{p'}{p}\right)^{\alpha} \frac{Q_1^{\rm sec}(p')D}{u_1^2}\left(1 + r^2\right)e^{-\chi(p,p')}\frac{dp'}{p'}, \qquad (3)$$

with $\alpha = 3r/(r-1)$ and $\chi \approx \alpha\left(\Gamma_1^{\rm inel}/\Gamma^{\rm acc}\right)[D(p) - D(p')]$, where $\Gamma^{\rm acc}$ is the acceleration rate. The first term of Equation (3) gives the acceleration spectrum of primary particles at the shock, of the form $f_0^{\rm pri} \sim p^{-\alpha}e^{-\chi}$. The second term describes the production and acceleration of CR fragments, and it is coupled with the equations of heavier nuclei. The amount of secondary nuclei production depends on the SNR properties via $n_1 D u_1^{-2}$. Their spectrum is of the form $f_0^{\rm sec} \sim f_0^{\rm pri} D(p) e^{-\chi} \propto p^{-\alpha+1}e^{-\chi}$, i.e., D times harder than the primary source spectrum. For having an efficient acceleration of all particles, the condition $\Gamma_1^{\rm inel} \ll \Gamma^{\rm acc}$ must be fulfilled in the whole momentum (or rigidity) range considered (Mertsch & Sarkar 2009). For Bohm-type diffusion ($D = \frac{R}{3B}$), this condition also can be expressed as $R \ll R^{\rm c} \sim \frac{3Bu_1^2}{20\, c\Gamma^{\rm inel}}$. At $R \gtrsim R^{\rm c}$, one has $\Gamma_1^{\rm inel} \gtrsim \Gamma^{\rm acc}$, i.e., destructive interactions dominate over acceleration. In the case of no interactions ($Q = 0$ and $\Gamma^{\rm inel/frag} = 0$), the usual DSA solution $f \propto p^{-\alpha}$ is recovered for primary nuclei, while the secondary CR production vanishes. The total CR flux produced by the SNR is obtained by integration in its volume:

$$S^{\rm snr}(p) = 4\pi p^2 e^{-p/p^{\rm max}} \int_0^{\tau^{\rm snr}u_2} 4\pi x^2 f_{2,j}(x, p)\, dx. \qquad (4)$$

The exponential cutoff $e^{-p/p^{\rm max}}$ is used to explicitly account for the maximum momentum attained by the SNR due to the finite time of the DSA process $\tau^{\rm snr}$, and it is assumed to occur at the same rigidity for all CRs in the accelerator: $R^{\rm max} \equiv p^{\rm max}/Z$. $R^{\rm max}$ can be roughly estimated from equating $\Gamma^{\rm acc}$ with $1/\tau^{\rm snr}$, which gives $\hat{R}^{\rm max} \sim 0.2\, Bu_1^2 c^{-1}\tau^{\rm snr}$, though it is usually left as a free parameter determined from the data (Kachelrieß et al. 2011; Serpico 2011). We stress that the steady-state description given here is an effective simplification of a more complex physical problem where the shock properties evolve with time.

For the Galactic propagation, we use an analytical approach of CR diffusion and nuclear interactions, where the effects of energy changes are disregarded (Maurin et al. 2001). The Galaxy is modeled as a disk of half-thickness h containing the ISM gas (number density $n_{\rm ism}$) and the CR sources. The disk is surrounded by a cylindric diffusive halo of half-thickness L and zero matter density. For each CR nucleus, the transport equation reads:

$$\frac{\partial N}{\partial t} = K\frac{\partial^2 N}{\partial z^2} - 2\, h\delta(z)\tilde{\Gamma}^{\rm inel} N + 2\, h\delta(z) S, \qquad (5)$$

Table 1
Source and Transport Parameter Sets

OSNR Parameters		Propagation Parameters	
u_1	5×10^7 cm s^{-1}	K_0	0.1 kpc^2 Myr^{-1}
B/κ_B	1 μG/16	δ	0.50
$\alpha_{\rm H}/\alpha_{Z>1}$	4.65/4.55	L	5 kpc
n_1	2 cm^{-3}	h	0.1 kpc
$R^{\rm max}$	1 TV	$n_{\rm ism}$	1 cm^{-3}
$\tau^{\rm snr}$	50 kyr	Φ	0.5 GV

where $N(z)$ is its number density as function of the z coordinate, K is the Galactic diffusion coefficient, and $\tilde{\Gamma}^{\rm inel} = \beta\, cn_{\rm ism}\sigma^{\rm inel}$ is the destruction rate in the ISM at velocity βc and cross-section $\sigma^{\rm inel}$. The source term S includes the SNR contributions, $S^{\rm snr}$, and the term for secondary production in the ISM from spallation of heavier (k) nuclei: $S^{\rm ism} = \sum_k \tilde{\Gamma}_k^{\rm frag} N_k$. The diffusion coefficient is taken as $K(R) = \beta K_0 \left(R/R_0\right)^{\delta}$, where K_0 expresses its normalization at $R_0 \equiv 4$ GV, and is spatially homogeneous. We solve Equation (5) for all nuclei (from Fe to H) after assuming stationarity ($\partial N/\partial t = 0$), boundary conditions ($N(\pm L) \equiv 0$), and continuity condition across the disk. The differential fluxes at Earth are given by $\phi(E) = \frac{\beta c}{4\pi} N_0(E)$, where N_0, evaluated at $z = 0$, is of the type $N_0 \approx S\left(\frac{K}{hL} + \tilde{\Gamma}^{\rm inel}\right)^{-1}$. The quantities N, K, S, and $\tilde{\Gamma}$ depend on energy or rigidity as well. To account for the solar modulation, we employ the *force-field* approximation (Gleeson & Axford 1968) using the parameter $\Phi = 500$ MV for a medium-level modulation strength.

3. RESULTS AND DISCUSSION

There are many parameters that determine the OSNR source spectra. We follow the benchmark model of Mertsch & Sarkar (2014), which provides good fits to the AMS leptonic data, assuming that the bulk of the $e^{\pm}$ flux is produced by this type of OSNR. All relevant parameters are listed in Table 1. In particular, we adopt $B = 1\ \mu$G, $R^{\rm max} = 1$ TV, $\kappa_B = 16$, and $u_1 = 5 \times 10^7$ cm s^{-1}, where κ_B parameterizes the deviation of $D(p)$ from the Bohm value due to magnetic damping. These values are typical for SNRs in their late evolutionary stages. The authors in Mertsch & Sarkar (2014) also considered scenarios with higher values of $R^{\rm max}$, fixed at 3 and 10 TV, that can, in principle, discriminate with e^+ data at higher energies. In Figure 1, we compare these predictions with the new high-energy data released by AMS (Accardo et al. 2014; Aguilar et al. 2014). The data suggest that models with high $R^{\rm max}$ ($\sim$10 TV or higher) are disfavored. We also note that the value $R^{\rm max} = 1$ TV is consistent with the naive estimate made from equating $\Gamma^{\rm acc}$ with $1/\tau^{\rm snr}$. At this point, it is clear that a pure OSNR scenario, which describes well the $\sim$GV–TV observations, cannot account for the CR hadronic flux observed at $\sim$TV–PV rigidities. This is also the rigidity region where the spectra are found to be harder. This consideration motivated us to introduce a second component for the CR hadron spectra at high energies, i.e., the GSNR component, representing the large-scale population of distant SNRs. Typical parameters for GSNRs with strong shock and amplified magnetic fields are $u_1 \sim 10^9$ cm s^{-1}, $B/\kappa_B \sim 100\ \mu$G, and $R^{\rm max} \sim 5$ PV. It is easy to see that from these values, GSNRs are unable to produce and accelerate secondary $e^{\pm}$ or Li–Be–B. Furthermore, the resulting CR spectra are totally insensitive to their exact values (and to the type of diffusion) so that the only relevant GSNR parameters are the source spectral indices. For both components, OSNR and GSNR, the slope α and their normalization are chosen to match the data on primary spectra after propagation. The source parameter α is degenerated with the transport parameter δ, but the latter can been tested against the B/C ratio. As in Mertsch & Sarkar (2014) and related works, for $Z = 1$, we use a source spectral index steeper by 0.1 compared to that of heavier nuclei. This is a known issue, possibly ascribed to an A/Z-dependent injection efficiency in SNR shocks (Malkov et al. 2012). The relative source abundances are those adopted from previous studies (Tomassetti 2012; Tomassetti & Donato 2012), and we use the same values for the two SNR components. The contributions of the two components, determined from the data, are taken as 85% for the OSNR and 15% for the GSNR flux at 1 GeV n^{-1} for all elements. Leptonic spectra from GSNRs are expected not to contribute significantly to the high-energy flux, which is the case if these sources are placed at distances of $d \gtrsim$ kpc (Delahaye et al. 2010). The data at $\gtrsim$TeV energies require the GSNR spectra to be harder than those from the OSNR: we adopt $\alpha_{\rm H} = 4.1$ and $\alpha_{Z>1} = 4.0$. This is in fact encouraging because the basic DSA predictions, supported by γ-ray observations of young SNRs, favor $\alpha \sim 4.0$–4.2 (Blasi 2013). With this setup, in Figure 2, we plot the model predictions for the Hand Hefluxes as function of kinetic energy per nucleon. The two components of the flux are shown, i.e., split as $\phi_{\rm H} = \phi_{\rm H}^{\rm O} + \phi_{\rm H}^{\rm G}$ and $\phi_{\rm He} = \phi_{\rm He}^{\rm O} + \phi_{\rm He}^{\rm G}$. The data are well described by the model, which interprets the TeV spectral hardening in terms of a smooth transition between the OSNR and the GSNR component, but the fine structures of the PAMELA data cannot be recovered. These sharp breaks also seem to be in contrast with the preliminary results of AMS . We eagerly await the AMS final results on H and He spectra at high energies, which will hopefully clarify how and where the spectral transition take places.

We now come to the B/C ratio. Figure 3 shows the B and C fluxes (top) and the B/C ratio (bottom) compared with recent data, including the new data from PAMELA (Adriani et al. 2014). The carbon flux, mostly primary, is also of the type $\phi_{\rm C} \approx \phi_{\rm C}^{\rm O} + \phi_{\rm C}^{\rm G}$. It also experiences a spectral hardening that is well reproduced by the model. The B spectrum, entirely secondary, can be ideally split into $\phi_{\rm B} = \phi_{\rm B}^{\rm O} + \phi_{\rm B}^{\rm ISM}$, where the first component is the one produced inside the OSNR, and the second arises in the ISM via collisions of heavier nuclei such as C, O, or Fe. Thus, the ISM component $\phi_{\rm B}^{\rm ISM}$ can be split again into $\phi_{\rm B}^{\rm ISM/O}$ (produced by collisions of OSNR-emitted nuclei) and $\phi_{\rm B}^{\rm ISM/G}$ (by GSNR-emitted nuclei). In previous OSNR-related works such as Cholis & Hooper (2014), the B/C ratio is always meant as $\left(\phi_{\rm B}^{\rm O} + \phi_{\rm B}^{\rm ISM/O}\right)/\phi_{\rm C}^{\rm O}$. Remarkably, while the ratio $\left(\phi_{\rm B}^{\rm O} + \phi_{\rm B}^{\rm ISM/O}\right)/\phi_{\rm C}^{\rm O}$ starts rising at $E \gtrsim 100$ GeV per nucleon (as expected from a pure OSNR scenario), the ratio of the two-component model $\phi_{\rm B}/\phi_{\rm C}$ decreases with energy in good agreement with the data. The trend of our B/C ratio is similar to the one from conventional propagation models (long-dashed line) where only the GNRS component is considered. This

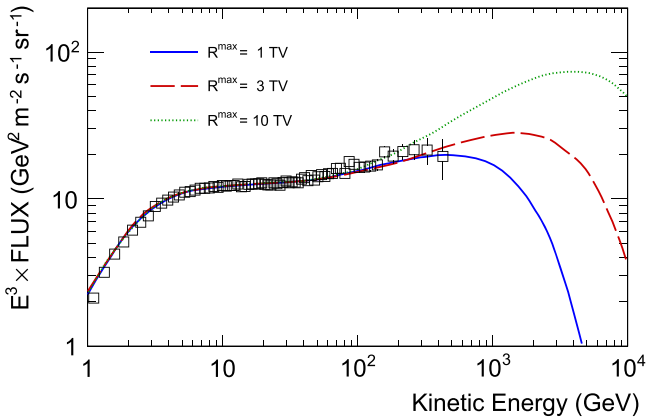

Figure 1. Energy spectrum of CR positrons multiplied by E^3. The three models of Mertsch & Sarkar (2014; lines) are compared with the new data from AMS (Aguilar et al. 2014).

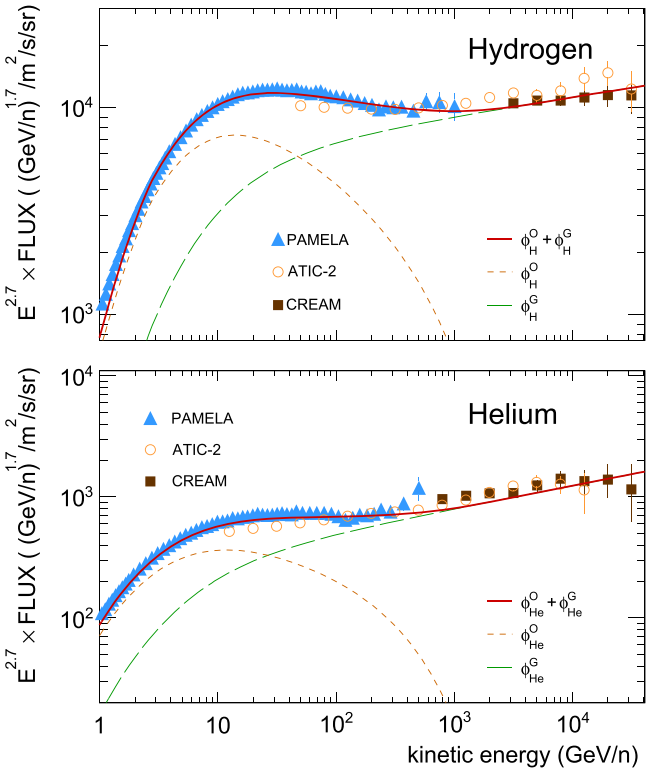

Figure 2. Energy spectra of H (top) and He (bottom) multiplied by $E^{2.7}$. The solid lines indicate the model calculations. The contribution arising from OSNR (short-dashed lines) and from GSNR (long-dashed lines) are shown. The data are from PAMELA (Adriani et al. 2011), ATIC-2 (Panov et al. 2009), and CREAM (Yoon et al. 2010).

effect can be understood from the top panel of the figure: at ∼100 GeV/nucleon, when the ONSR component of B would become relevant enough to provide a signature (i.e., $\phi_B^O \gtrsim \phi_B^{ISM/O}$), the total fluxes of B and C are both dominated by the GSNR components, $\phi_B^{ISM/G}$ and ϕ_C^G, respectively. Thus, in our two-component scenario, the B/C ratio does not constrain secondary production in the SNR, as the presence of the GSRN component breaks the connection between the positron fraction and the secondary-to-primary nuclear ratios. We have tested the calculation using different values of R^{max}. However, due to a degeneration with the OSNR parameter α,

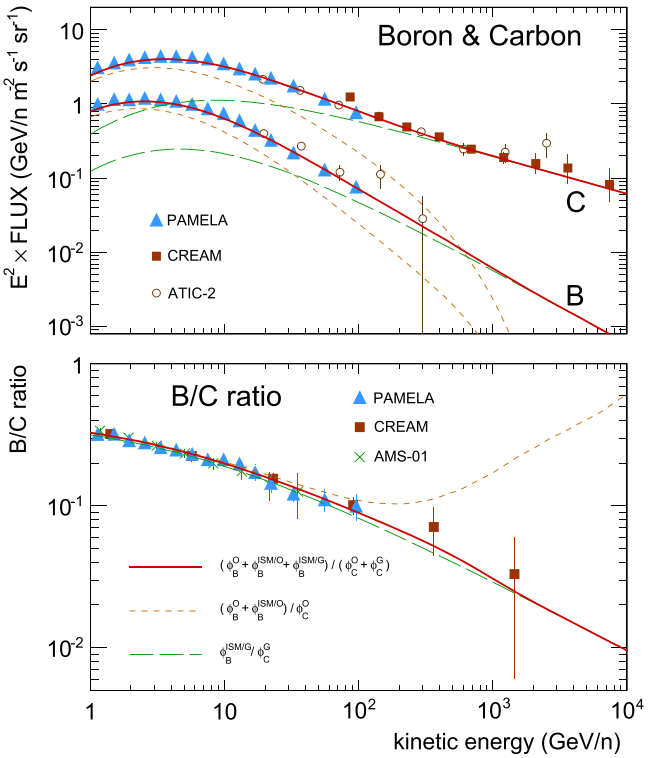

Figure 3. Top: CR energy spectra of B and C multiplied by E^2. Bottom: B/C ratio. The lines indicate the model calculations. In the top panel, the B components are for $\phi_B^O + \phi_B^{ISM/O}$ (short-dashed line) and $\phi_B^{ISM/G}$ (long-dashed line) and their sum (solid line). The C components are for ϕ_C^O (short-dashed line) and ϕ_C^G (long-dashed line) and their sum (solid line). The data are from and PAMELA (Adriani et al. 2014), CREAM (Yoon et al. 2010), AMS -01 (Aguilar et al. 2010), and ATIC-2 (Panov et al. 2009).

the parameter R^{max} cannot be constrained much within the precision of the data. Our results for the B/C ratio seem to be quite robust: once accounting for the GSNR component, it decreases with energy as $\sim E^{-\delta}$ (giving only little wiggles around the energy $E \approx R^{max}/2$; see Figure 3). For $R^{max} \sim 1$ TV or less, the spectra of H and He experience deviations from the power-law behavior below the TeV region that should be measurable by AMS .

4. CONCLUSIONS

Our work is motivated by two outstanding problems in CR physics: the origin of the rise in the positron fraction at $E \gtrsim 10$ GeV and the nature of the ∼TeV spectral hardening in CR hadrons. We revisited the ONSR scenario, proposed for the positron fraction anomaly, in order to account for the high-energy observations of CR hadrons and nuclei. In OSNR models, secondary particles such as positrons and light nuclei are produced and accelerated inside SNRs via hadronic interactions. In order to be able to match the $e^{\pm}$ data, these old SNRs must have particular properties in terms of environmental parameters (such as strongly damped magnetization or relatively high gas density) and predict features in the B/C ratio that are not observed. In this Letter, we have argued that the OSNR scenario is incomplete for explaining the flux of CR hadrons at ∼TeV–PeV energies. The OSNR can account for the leptonic flux and for the GeV–TeV production of CR hadrons, but the flux at higher energies has to be provided by a population of distant and young sources that are able to

efficiently accelerate CRs up to the knee. These sources are unable to produce secondary CRs (due to magnetic field amplification), and they do not contribute significantly to the high-energy leptonic flux (due to the large distance). Within this picture, the spectral hardening of CR hadrons is interpreted as a signature of the transition between the local OSNR component and the Galactic ensemble. The spectra of all primary nuclei are predicted to harden. Taking into account the contribution of the two populations, we found that the predicted B/C ratio shows no prominent signatures; it decreases with energy in accordance with the existing data. In conclusion, this generalized scenario may explain the absence of signatures in the B/C ratio while accounting for the observed signatures in primary CR hadrons. A quantitative inspection will be done with a proper modeling of leptonic and hadronic spectra arising from a realistic time-space distribution of their sources. To achieve this goal, it will be crucial to have precision data on CR protons nuclei in the energy region where the spectral transition takes place.

N.T. acknowledges the support of the Labex grant ENIGMASS. The work of F.D. is supported by the *Strategic Research Grant: Origin and Detection of Galactic and Extragalactic Cosmic Rays* funded by Torino University and Compagnia di San Paolo and by the research grant *Theoretical Astroparticle Physics* No. 2012CPPYP7 under the program PRIN-2012 funded by the MIUR, Italy.

REFERENCES

Accardo, L., Aguilar, M., Aisa, D., et al. 2014, PhRvL, 113, 121101
Adriani, O., Barbarino, G. C., Bazilevskaya, G. A., et al. 2014, ApJ, 791, 93
Adriani, O., Barbarino, G. C., Bazilevskaya, G. A., et al. 2011, Sci, 332, 6025
Adriani, O., Barbarino, G. C., Bazilevskaya, G. A., et al. 2009, Natur, 458, 607
Aguilar, M., Aisa, D., Alvino, A., et al. 2014, PhRvL, 113, 121102
Aguilar, M., Alberti, G., Alpat, B., et al. 2013, PhRvL, 110, 141102
Aguilar, M., Alcaraz, J., Allaby, J., et al. 2010, ApJ, 724, 329
Bernard, G., Delahaye, T., Salati, P., & Taillet, R. 2013, A&A, 555, A48
Blasi, P. 2013, A&ARv, 21, 70
Blasi, P. 2009, PhRvL, 103, 051104
Blasi, P., Amato, E., Serpico, P. D., et al. 2012, PhRvL, 109, 061101
Cholis, I., & Hooper, D. 2014, PhRvD, 89, 043013
Delahaye, T., Lavalle, J., Lineros, R., Donato, F., Fornengo, N., et al. 2010, A&A, 524, A51
Gleeson, L. J., & Axford, W. I. 1968, ApJ, 154, 1011
Kachelrieß, M., Ostapchenko, S., Tomàs, R., et al. 2011, ApJ, 733, 119
Maurin, D., Donato, F., Taillet, R., Salati, P., et al. 2001, ApJ, 555, 585
Malkov, M. A., Diamond, P. H., Sagdeev, R. Z., et al. 2012, PhRvL, 108, 081104
Mertsch, P., & Sarkar, S. 2009, PhRvL, 103, 081104
Mertsch, P., & Sarkar, S. 2014, PhRvD, 90, 061301
Panov, A. D., Adams, J. H., Ahn, H. S., et al. 2009, BRASP, 73, 564
Ptuskin, V. S., Zirakashvili, V., Eun-Suk, S., et al. 2013, ApJ, 47, 763
Serpico, P. 2012, APh, 39, 2
Strong, A. W., Moskalenko, I. V., Ptuskin, V. S., et al. 2007, ARNPS, 57, 285
Taillet, R., & Maurin, D. 2003, A&A, 402, 971
Thoudam, S., & Horandel, J. 2013, MNRAS, 435, 2532
Tomassetti, N. 2012, ApJL, 752, L13
Tomassetti, N., & Donato, F. 2012, A&A, 544, A16
Vladimirov, A. E., Jóhannesson, G., Moskalenko, I. V., & Porter, T. A. 2012, ApJ, 752, 68
Yoon, Y. S., Ahn, H. S., Allison, P. S., et al. 2010, ApJ, 715, 1400